Thermochimica Acta, 102 (1986) 303–310
Elsevier Science Publishers B.V., Amsterdam – Printed in The Netherlands

STRUCTURAL AND TEXTURAL CHARACTERIZATION OF ALUM-DERIVED ACTIVE ALUMINA

E. ESCALONA PLATERO, J.M. RUBIO GONZÁLEZ and C. OTERO AREÁN

Departamento de Química Inorgánica, Universidad de Oviedo, 33071 Oviedo (Spain)

(Received 26 November 1985)

ABSTRACT

Active alumina prepared by thermolysis of ammonium alum has been characterized by X-ray diffraction and nitrogen adsorption at 77 K. The material was found to have a defective spinel-type structure in which 2 2/3 octahedral cation sites per unit cell are vacant. Specific surface area was found to be 170 m^2 g^{-1}. This high surface area was not altered on prolonged calcination at 773 K. However, firing at 1173 K led to a final equilibrium value of 90 m^2 g^{-1}. Pore-size distribution was shown to be unimodal, the most frequent pore radius appearing at 10 nm.

INTRODUCTION

Aluminas are used widely, either as single materials or in multicomponent systems, for preparing refractories, fine ceramics, abrasives, catalysts or catalyst-supports. For some of these applications materials with a high specific surface area (active aluminas) are required, either as end products or precursors. Surface properties and reactivity of these aluminas are determined largely by their crystal structure and porous texture, which also condition the corresponding thermal behaviour during sintering or in high-temperature catalytic processes.

Precursor materials for the preparation of active aluminas are usually aluminium hydroxides [1–6] or sulphates [7–11]. Aluminas prepared by the controlled thermolysis of aluminium hydroxides have been extensively studied [1–6,12,13] but thermal decomposition of aluminium oxosalts has so far received less attention, particularly concerning the textural properties of the products obtained. However, some recent studies [10,14,15] have shown that thermolysis of aluminium sulphates can lead to high surface area aluminas with potential use as adsorbents and catalysts.

The present work reports on the crystal structure and surface texture of active alumina prepared by thermal decomposition (at 1173 K) of ammonium alum, and on the thermal behaviour of this material during subsequent heat treatments. The results are compared with those corresponding to active aluminas derived from aluminium hydroxides [1,6,16–19].

0040-6031/86/$03.50

EXPERIMENTAL

Ammonium alum, supplied by Koch-Light Laboratories with a nominal purity of 99.97%, was subjected to thermolysis for 6 h at 1173 K. The resulting material, termed AA1173, was divided into separate portions which were subjected to different heat treatments in order to investigate the evolution of crystal structure, specific surface area and porous texture. These heat treatments were as follows: (i) 6 h at 1273 K (sample AA1273), (ii) 300 h at 773 K (sample AA773) and (iii) cumulative calcinations at 1173 K during increasing time periods, as described in the next section. All calcinations, as well as the initial thermolysis, were carried out in an electric furnace preheated to the desired temperature, the sample being contained in a platinum crucible and exposed to the atmosphere. A temperature controller ensured that temperature fluctuations never exceeded ±10 K. At the end of each calcination period the sample was withdrawn from the furnace and allowed to quench in air.

X-ray powder diffractograms (Cu K_α radiation) were obtained with an X-ray diffractometer equipped with a graphite crystal monochromator and scintillation counter. For samples AA1173 and AA1273 diffraction intensities were determined with the same experimental arrangement.

Specific (BET) surface area, pore volume and pore size for each sample were determined from the corresponding nitrogen adsorption–desorption isotherm (77 K). These isotherms were obtained using a volumetric apparatus of conventional design; nitrogen N39 was used as the adsorptive and helium N45 for calibration of dead volumes. Prior to the determination of each isotherm the corresponding sample was outgassed at 423 K for 2 h, in a dynamic vacuum of 10^{-2} Pa.

RESULTS AND DISCUSSION

Structural characterization

Relevant portions of the X-ray diffractograms corresponding to samples AA1173 and AA1273 are shown in Fig. 1. Table 1 shows that the observed *d*-spacings and diffraction intensities agree with those given by the ASTM for γ-alumina [20]. No other crystalline phases were apparent. In particular, neither X-ray diffraction nor IR spectroscopy (KBr-pressed disks) showed any traces of undecomposed ammonium alum.

It should be pointed out that discrimination between γ- and η-alumina is not unambiguous, especially in the case of poorly crystallized materials. Both phases have a lattice closely related to that of spinel [6,21,22], the corresponding X-ray diffraction patterns are very similar and differ only in the following features [6,23]: (i) the 198 pm band is doubled (because of

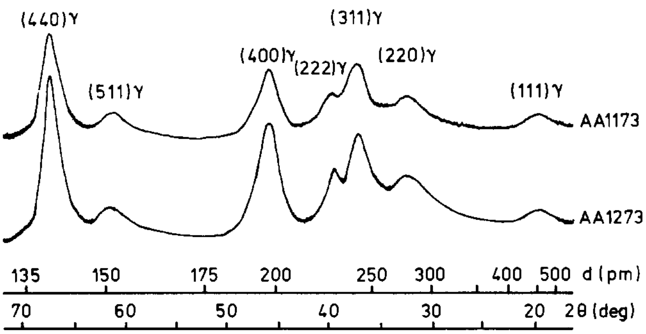

Fig. 1. X-ray diffraction patterns of samples AA1173 and AA1273.

tetragonal distortion) in the case of γ-alumina, whilst that of η-alumina shows only an asymmetric profile; (ii) the 460 pm band of γ is very broad, whereas that of η is sharp with a broadened base. This last criterion led to the assignment of the γ-modification for samples AA1173 and AA1273. The first criterion cannot be used because of severe line broadening, which precludes observation of any splitting of the 198 pm band. Sato et al. [24] in a study of the thermolysis of ammonium alum have also concluded that the material obtained is γ-alumina.

The structure of γ-alumina can be described as a defective spinel [25] in which 21 1/3 of the available 24 cation sites (per unit cell) are occupied by aluminium ions and 2 2/3 are left vacant. For γ-alumina derived from aluminium hydroxide, Verwey [18] deduced that the 2 2/3 vacancies are on the octahedral positions whilst the 8 tetrahedral positions and the remaining 13 1/3 octahedral sites are taken by Al^{3+} ions. This corresponds to the structural notation $Al_8(Al_{13\ 1/3}\square_{2\ 2/3})O_4$ where parentheses enclose the octahedral cation sites. In a study of mixed crystals of spinel ($MgAl_2O_4$) and γ-alumina, Jagodszinski and Saalfeld [26] also found that the 2 2/3 vacant cation positions are probably in the octahedral sublattice. However, from a

TABLE 1

Crystal data for sample AA1173

d (pm)		I/I_0		(*hkl*)
Observed	ASTM (γ-Al_2O_3)	Observed	ASTM (γ-Al_2O_3)	
455	456	20	40	(111)
277	280	20	20	(220)
240	239	80	80	(311)
228	228	30	50	(222)
198	197.7	100	100	(400)
152	152.0	30	30	(511)
139.8	139.5	100	100	(440)

later investigation on γ-alumina obtained from boehmite, Saalfeld and Mehrotra [27] concluded that, in this case, the octahedral sublattice is fully occupied, whereas the tetrahedral sublattice has vacant cation sites.

From the intensities of the (111), (220, 311, 222, 400), (511, 440), (444), (553, 731, 800) and (840) X-ray diffraction lines we have determined the cation distribution of samples AA1173 and AA1273, using a computational method previously described [28,29]. Both γ-aluminas were found to have the distribution $Al_8(Al_{13\ 1/3}\ \square_{2\ 2/3})O_4$, i.e., the vacancies are on the octahedral sublattice. In principle it could be expected that, because of the entropy contribution to the free energy, a certain randomization of the vacancies between the tetrahedral and octahedral sublattices could be observed on raising the temperature (from 1173 to 1273 K). However, within the limits of the present research, no temperature-dependent redistribution was found. Possible randomization at temperatures significantly higher than 1273 K is difficult to investigate because it has been shown [14] that at 1323 K there is a partial transformation into δ-alumina, followed by θ and finally α (at 1373 K). This complicates the analysis of diffraction intensities needed for determining cation distribution.

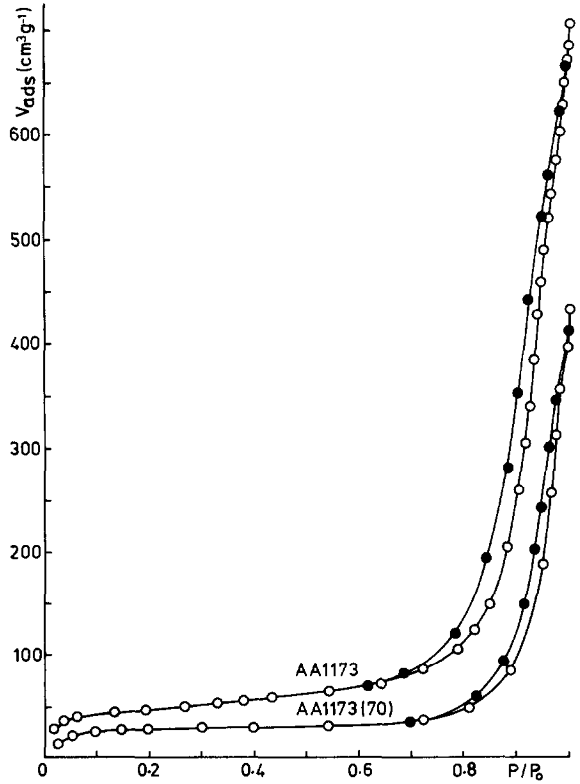

Fig. 2. Nitrogen adsorption (O)/desorption (●) isotherms at 77 K.

Textural characterization

The nitrogen adsorption-desorption isotherm of sample AA1173, shown in Fig. 2, is akin to type IV of the BDDT classification [30] and the hysteresis loop corresponds to type A of the classification proposed by de Boer [31]. These facts suggest that the γ-alumina obtained by thermolysis of ammonium alum is a mesoporous solid, the pore texture of which conforms to a geometric model of tubular pores with widened parts (or wide-necked ink-bottle-shaped pores). The absence of significant microporosity, suggested by the shape of the isotherm, is confirmed by the fact that the corresponding V_a–t plot [32,33], shown in Fig. 3, extrapolates through the origin. The observed increasing slope of this t-plot in the high t-value region supports the above-mentioned assignment of pore shape [34].

Specific (BET) surface area, pore size and pore volume of sample AA1173, determined from the adsorption isotherm, are presented in Table 2. The surface area was calculated by taking the value of 0.162 nm^2 for the surface covered by one nitrogen molecule. The porous texture was analysed following the Pierce method [35], with the equation of Halsey [36] for multilayer thickness. For monolayer thickness the value of 354 pm was taken. The

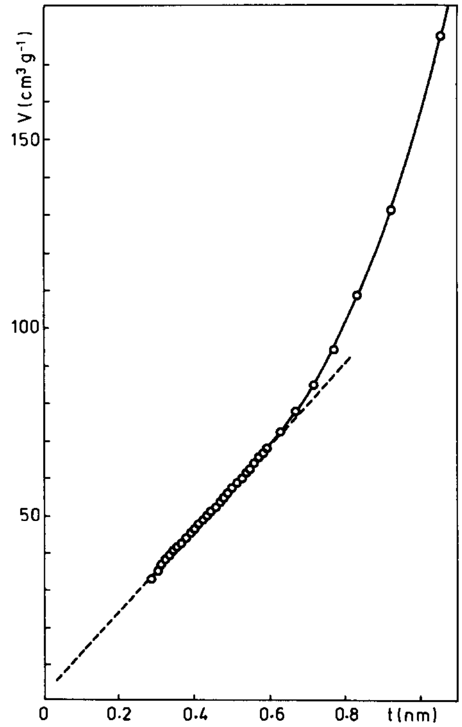

Fig. 3. V_a–t plot for sample AA1173.

TABLE 2

Textural parameters of different alumina samples

Sample	Calcination temperature (K)	Calcination time (h)	S_{BET} ($m^2 g^{-1}$)	r_p (nm)	V_p ($cm^3 g^{-1}$)
AA1173	–	–	170	10	1.10
AA773	773	300	170	–	–
AA1173(12)	1173	12	140	11	1.00
AA1173(25)	1173	25	115	–	–
AA1173(40)	1173	40	110	12	0.70
AA1173(70)	1173	70	90	13	0.67
AA1173(130)	1173	130	90	13	0.66

analysis was applied to the adsorption branch of the isotherm, which is to be preferred to the desorption branch for type IV isotherms [34,37]. The resulting pore-size distribution curve was unimodal and relatively narrow, as shown in Fig. 4.

To check the reproducibility of the preparation method, two more portions of the same ammonium alum were subjected to thermolysis under the same experimental conditions as described for sample AA1173. Surface area and textural parameters determined from the corresponding nitrogen sorption isotherms, resulted to be well within ±3% of the values reported in Table 2 for AA1173. It is not often found that thermolysis of precursors leads to active solids with so highly reproducible textural parameters. We believe that in the present case reproducibility is facilitated by the fact that ammonium alum melts before thermal decomposition. This eliminates sources of variability such as structure-sensitive processes, particle size and compactness of the starting material.

Thermal treatments

In order to investigate the thermal behaviour of the γ-alumina obtained, concerning the relevant textural parameters, separate portions of sample

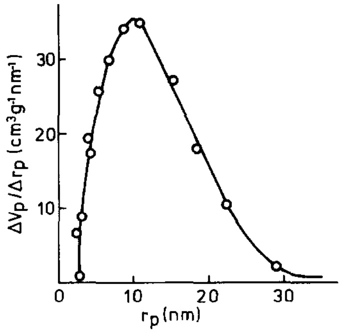

Fig. 4. Pore radii distribution of sample AA1173.

AA1173 were calcined (i) for 300 h at 773 K; and (ii) for increasing time periods at 1173 K, as shown in Table 2. From the corresponding nitrogen adsorption isotherms, textural parameters were calculated as described previously for sample AA1173.

Prolonged calcination (300 h) at 773 K did not alter the surface area, as shown in Table 2 (sample AA773). This thermal stability contrasts with the behaviour often shown by active aluminas prepared by the controlled thermolysis (at 500–600 K) of aluminium hydroxides. Materials prepared by this last method usually show surface areas of about 250 m^2 g^{-1}; however, the corresponding pore spectrum is frequently very broad [1,6,16,17] and a substantial part of the internal area corresponds to micropores. This micropore system collapses when the materials are heated at about 800 K, with concomitant alteration of surface area and pore texture [17]. It is also relevant to point out that the thermal decomposition of aluminium hydroxides tends to produce active aluminas with slit-shaped pores [6,16], as compared with the cylindrical pores formed in alum-derived materials.

A portion of sample AA1173 was calcined at 1173 K for increasing time periods; samples thus obtained are termed AA1173(x) where x denotes cumulative calcination time (in h, see Table 2). Nitrogen sorption isotherms of these samples were also type IV with type A hysteresis loops, as shown for AA1173(70) in Fig. 2. Computation of the corresponding textural parameters has shown that isothermal calcination at 1173 K causes a moderate thermal sintering process in which surface area and pore volume are gradually reduced and the mean pore radius is increased, as shown in Table 2. It is known [38,39] that decrease in surface area on isothermal sintering of a porous solid tends towards a final equilibrium value determined by the initial physical condition of the material and the temperature of the experiment. This is the trend shown by the data reported in Table 2 where, on prolonged calcination, specific surface area stabilizes at 90 m^2 g^{-1}.

REFERENCES

1 J.W. Newsome, H.W. Heiser, A.S. Rusell and H.C. Stumpf, ALCOA Res. Lab. Tech. Pap. No. 10, Aluminum Company of America, Pittsburgh, PA, 1960.
2 D.S. Maciver, H.H. Tobin and R.T. Barth, J. Catal., 2 (1963) 485.
3 B.C. Lippens and J.H. de Boer, J. Catal., 3 (1964) 44.
4 D. Aldcroft, G.C. Bye, J.G. Robinson and K.S.W. Sing, J. Appl. Chem., 18 (1968) 301.
5 M.A. Vicarini, G.A. Nicolaon and S.J. Teichner, Bull. Soc. Chim. Fr., (1970) 431.
6 B.C. Lippens and J.J. Steggerda, in B.G. Linsen (Ed.), Physical and Chemical Aspects of Adsorbents and Catalysts, Academic Press, New York, 1970.
7 D.W. Johnson and F.J. Schnettler, J. Am. Ceram. Soc., 53 (1970) 440.
8 E. Kato, K. Daimon, A. Yamaguchi and T. Yamada, Yogyo Kyokai Shi, 85 (1977) 134.
9 E. Escalona Platero, C. Otero Areán and A. Mata Arjona, Mater. Chem. Phys., 9 (1983) 493.
10 M.D. Sacks, T.Y. Tseng and S.Y. Lee, Am. Ceram. Soc. Bull., 63 (1984) 301.

11 F.W. Dynys and J.W. Halloran, J. Am. Ceram. Soc., 65 (1982) 442.
12 J. Rouquerol, F. Rouquerol and M. Ganteaume, J. Catal., 57 (1979) 222.
13 T. Kotanigawa, M. Yamamoto, M. Utiyama, H. Hattori and K. Tanabe, Appl. Catal., 1 (1981) 185.
14 E. Escalona Platero, C. Otero Areán and A. Mata Arjona, An. Quim., 80 (1984) 294.
15 C. Otero Areán and E. Escalona Platero, Adsorption Sci. Technol., 1 (1984) 159.
16 B.C. Lippens, Thesis, Delft University of Technology, The Netherlands, 1955.
17 J.H. de Boer, Angew. Chem., 70 (1985) 383.
18 E.J.W. Verwey, Z. Kristallogr., 91 (1935) 317.
19 S. Wilson and M.H. Stacey, J. Colloid Interface Sci., 82 (1981) 507.
20 ASTM Powder Diffraction File, Card No. 10-425.
21 G. Yamaguchi and H. Yanagida, Bull. Chem. Soc. Jpn., 35 (1962) 1896.
22 B.C. Lippens and J.H. de Boer, Acta Crystallogr., 17 (1964) 1312.
23 C.A. Spitler and S.S. Pollack, J. Catal., 69 (1981) 241.
24 T. Sato, F. Ozawa and S. Ikoma, J. Appl. Chem. Biotechnol., 28 (1978) 811.
25 R.C. Evans, Crystal Chemistry, Cambridge University Press, Cambridge, 1966.
26 H. Jagodszinski and H. Saalfeld, Z. Kristallogr., 110 (1958) 197.
27 H. Saalfeld and B. Mehrotra, Ber. Dtsch. Keram. Ges., 42 (1965) 161.
28 H. Furuhashi, M. Inagaki and S. Naka, J. Inorg. Nucl. Chem., 35 (1973) 3009.
29 J.M. Rubio González and C. Otero Areán, J. Chem. Soc., Dalton Trans., (1985) 2155.
30 S. Brunauer, L.S. Deming, W.S. Deming and E. Teller, J. Am. Chem. Soc., 62 (1940) 1723.
31 J.H. de Boer, in D.H. Everett and F.S. Stone (Eds.), The Structure and Properties of Porous Materials, Butterworths, London, 1958.
32 B.C. Lippens, B.G. Linsen and J.H. de Boer, J. Catal., 3 (1964) 32.
33 B.C. Lippens and J.H. de Boer, J. Catal., 4 (1965) 319.
34 J.C.P. Broekhoff and B.G. Linsen, see ref. 6, pp. 1–62.
35 C. Pierce, J. Phys. Chem., 57 (1953) 149.
36 G.D. Halsey, J. Chem. Phys., 16 (1948) 931.
37 A. Mata Arjona, J.B. Parra Soto and C. Otero Areán, Stud. Surf. Sci. Catal., 10 (1982) 175.
38 D. Dollimore, Thermochim. Acta, 38 (1980) 1.
39 M.A. Villa García, E. Escalona Platero, J.M. Fernández Colinas and C. Otero Areán, Thermochim. Acta, 90 (1985) 195.